Research Article Vol. 32, No. 13 / 17 Jun 2024 / Optics Express 23597

Optics EXPRESS

Individual differences in color matches and cone spectral sensitivities in 51 young adults

KEYU SHI,[1] MING RONNIER LUO,[1,*] ANDREW T. RIDER,[2] SIYUAN SONG,[1] TINGWEI HUANG,[3] AND ANDREW STOCKMAN[1,2]

[1]State Key Laboratory of Extreme Photonics and Instrumentation, Zhejiang University, Hangzhou, China
[2]Institute of Ophthalmology, University College London, EC1 V 9EL London, United Kingdom
[3]Thousand Lights Lighting (Changzhou) Limited, Changzhou, China
[*]m.r.luo@zju.edu.cn

Abstract: Forty-six young adult observers with normal color vision (plus five from an earlier study) made a series of color matches using a new LED-based, multi-wavelength visual trichromator. Thirteen LED lights of different wavelengths were combined to produce 11 triplets of lights that observers were asked to match to a white reference light of 7500 K over visual angles of either 2° or 10°. Matches were initially made by asking observers to adjust the intensities of the three lights making up each triplet. As the experiment progressed, a more intuitive matching procedure was developed. By transforming the triplet of lights into CIELAB space, observers adjusted colors using lightness (L*), redness-greenness (a*), and blueness-yellowness (b*) to make the match with white. The new procedure proved easier for observers and reduced the inter- and intra-observer variability. Given that each of the 11 matches to the reference white for a given observer (obtained by either method) should produce identical L-, M- and S-cone excitations, we were able to use the matches to infer the individual cone spectral sensitivities for each observer and thus estimate the range of individual differences across our 51 observers. By applying a model of the CIEPO06 standard LMS observer, the photopigment, macular and lens optical densities and the L- and M-cone photopigment spectral shifts that best equated the three-cone excitations across the 11 matches were found for each observer. The individual differences were consistent with the CIEPO06 observer except for a 3 nm shift of the M-cone photopigment to longer wavelengths and a slightly denser 2-deg macular pigment density.

1. Introduction

The initial stage of human color vision depends on the spectral sensitivities of the long- (L-), middle- (M-), and short- (S-) wavelength-sensitive cone types. In 2006, the CIE adopted a new physiological observer model (hereafter refer to as CIEPO06) that defines the standard or mean L-, M- and S-cone spectral sensitivities (measured with respect to light entering the eye at the cornea) for 2° (small-field) and 10° (large-field) fields of view (FOV) [1,2]. The new CIEPO06 standard is based almost entirely on the work of Stockman and Sharpe [3] and Stockman, Sharpe & Fach [4], who made cone spectral sensitivity measurements in a large group of genotyped dichromatic, monochromatic and color normal observers. Stockman & Sharpe defined their cone spectral sensitivities as linear transformations of the mean 10° color matching functions (CMFs) measured by Stiles-Burch in 47 observers [5,6]. A 2° version was generated by appropriately adjusting the macular and photopigment optical densities, all of which are higher in and around the fovea.

Standard observers are useful for modelling and predicting the color vision of a typical color-normal observer. However, they are less useful for color-normal observers who differ significantly from the mean observer because of individual differences in the macular or lens optical densities, photopigment optical densities or spectral shifts of the underlying cone photopigment spectra [7]. These individual differences, which are found in observers with ostensibly "normal" color vision,

#523287 https://doi.org/10.1364/OE.523287
Journal © 2024 Received 28 Feb 2024; revised 30 May 2024; accepted 30 May 2024; published 12 Jun 2024

Optics EXPRESS

can cause characteristic changes in the shapes of the corneally measured L-, M- and S-cone spectral sensitivities (also known as the LMS cone fundamentals or CMFs). These differences are also, of course, apparent in other CMFs such as the XYZ or RGB CMFs, which are linear transformations of LMS. Figure 1 shows the 47 individual sets of 10° RGB CMFs measured by Stiles & Burch upon which the CIEPO06 standard is based. The variability in Fig. 1 provides a good indication of the variability that should be expected in a population of color normal observers. Webster & MacLeod [8] analyzed the sources of variability in these data and attributed them to lens, macular, and photopigment optical densities and photopigment spectral shifts. In general, interpreting individual differences is most easily done when the data are in LMS form where they can be directly related to the underlying physiology rather than in the RGB form shown in Fig. 1 (or in the XYZ form).

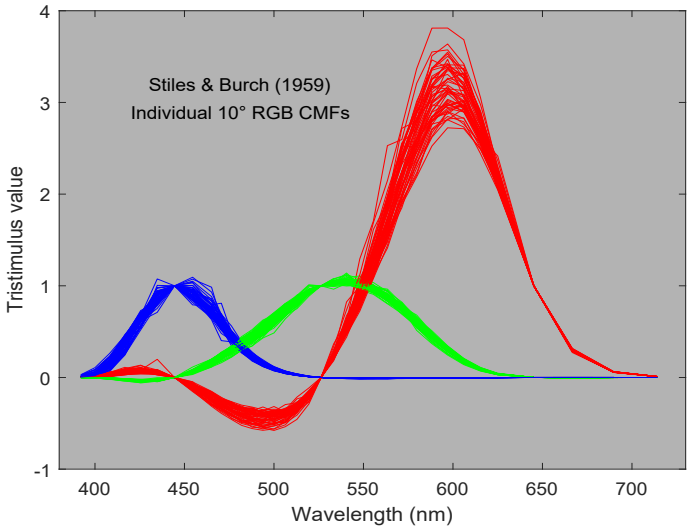

Fig. 1. Individual 10° RGB color matching functions of the 47 observers used by Stiles & Burch (1959).

Several recent studies have used devices with up to six primary lights principally to investigate the effects of individual differences on cross-media color matches [9–12]. These matches, however, unlike those in this study, were not used to estimate the cone fundamentals of individual observers. An exception was the study by Asano *et al.* [13], but their analysis gave unexpected values for some individual differences.

The need to account for individual differences has become increasingly urgent with the development of new display technologies and the use of more narrow-band, spectrally-pure display primaries, the color appearances of which are more affected by individual differences than broad-band primaries [14–16]. This paper is the second in a series of papers in which we measure color matches and from them infer individual differences in the underlying cone spectral sensitivities. As reported in our first paper [17], a new LED-based visual trichromator, called LEDMax, was developed, with which we acquired color matching data from five experienced observers each of whom made repeated matches between triplets of primaries and a white standard. A parametric model of cone spectral sensitivities based on CIEPO06 was then applied to generate estimates of each individual's L-, M- and S-cone spectral sensitivities from these matches. Inter- and intra-observer variabilities were found to be small.

The LEDMax was used to obtain color matching data from a much larger group of fifty-one observers. In addition, we tested two methods of adjusting the lights in the trichromator to

Optics EXPRESS

make color matches. We either allowed observers to independently adjust the intensity of the three matching test lights to make a match to the white, or alternatively we converted the three lights into CIELAB coordinates and allowed observers to adjust the lightness, redness-greenness, and blueness-yellowness of the combined lights to make a match to the white. We found that both methods produce similar results, but the Lab method has lower inter- and intra-observer variability.

2. Methods

2.1. Color matching

The traditional method of measuring CMFs is to ask observers to match test lights of variable wavelength (λ) by mixing three primary lights, typically red (R), green (G) and blue or violet (B). Observers are presented with a half field illuminated by the test light and one of the three primaries, and a second half field illuminated by the two remaining primaries. Which of the three primaries are added to the test light depends on test wavelength, as can be seen by where the relevant CMF is negative in Fig. 1: G is negative at short wavelengths, R at middle wavelengths, and B at long wavelengths (the scale on Fig. 1 obscures the small negative B lobe). Observers then vary the intensity of the R, G and B lights until both sides match. This method is known as the maximum saturation method and was used by Stiles & Burch [5], and also by Guild [18] and Wright [19] on whose results the CIE 1931 CMFs are based. An alternative method is Maxwell's method [20], in which a standard reference white (W) is shown in one half-field, and a combination of three lights [usually two of the three primaries (R, G or B) and one variable wavelength test light (λ)] is shown in the other half-field. Observers then vary the intensities of the three lights to match the reference white. In Maxwell's method, the matched fields always appear white, whereas in the maximum saturation method the color of the matched fields changes with test wavelength. A potential problem with the maximum saturation method is that the experimental conditions are not fixed across test wavelength. Nonetheless, if color matching additivity holds [21], there should be no differences between the resulting CMFs. However, chromaticity coordinates measured by Crawford [22] using Maxwell's method show clear discrepancies when compared with those measured using the maximum saturation method (see his Figs. 3 and 4) particularly for wavelengths between his blue (460 nm) and green (530 nm) primaries. The discrepancies show that Maxwell's method requires more intense red (650 nm) and less intense blue primaries to complete the match than the maximum saturation method for these wavelengths. Comparable discrepancies have been found by Wyszecki in pilot data first reported in Wyszecki & Stiles [23] (see their Figs. 4(5.6.6) and 5(5.6.6)) and later by Zaidi, who concluded it was due to nonlinear post-receptoral interactions [24]. The Maxwell method is preferred since the state of adaptation at the match is held constant, but the discrepancies may lead to small inconsistencies between our matches and the CIEPO06 matches and CIE matches.

2.2. Apparatus

A multi-primary visual trichromator named LEDMax was developed for the color matching. The system has been described in detail in our previous paper [17]. Briefly, a pair of LED illuminators each illuminated by up to 18 LEDs with center wavelengths ranging from 400 to 700 nm uniformly lit two side-by-side semi-circular apertures. Two sets of apertures could be fixed to the front of the device, subtending either 2° or 10° depending on the FOV for the matches.

The illuminators can be controlled by the observers using a color adjustment panel. In these experiments, observers adjusted the color appearance of one semicircular field to match the other fixed standard white half-field. System performance and calibration details are described in detail in our previous paper [17]. See, in particular, Figs. 2 and 3 and Table 1 of our previoius paper [17].

Optics EXPRESS

2.3. Triplets chosen to match the white reference

The fixed reference white half-field, which was made up of a mixture of 640, 530, and 445-nm lights (close to the wavelengths used by Stiles and Burch: 645, 526 and 444 nm), was set to a correlated color temperature (CCT) of 7500 K (following Asano et al. 2016 [25]) and a luminance of 120 cd/m^2 to rule out rod intrusion. In the mixture half-field, we used either the same LEDs as the reference or we replaced one of the reference LEDs with one of 10 LEDs of different wavelength to produce a total of 11 triplets of lights that were to be matched to the reference white. This leave-one-out procedure mimics that of traditional color matching studies. We are currently studying whether other procedures might prove to be more efficient. Five of the available 18 LEDs in the device were not used in this study as they were too dim, too broadband or located at the extremes of visible spectrum. Table 1 list the 11 triplets used to in mixture half-field. Details of the lights are given in our previous paper. The first set is called the standard because the same triplet was used in the standard half-field to produce the white reference. Table 1 list the 11 triplets used to in mixture half-field. Details of the lights are given in our previous paper.

Table 1. The 11 different triplets used in the mixture half-field.

Triplets	R (nm)	G (nm)	B (nm)
Standard	640	530	445
1	640	530	430
2	640	530	460
3	640	530	475
4	640	505	445
5	640	545	445
6	640	560	445
7	595	530	445
8	605	530	445
9	660	530	445
10	675	530	445

Observers were first presented with a white standard half-field on the right, and were asked to match it by varying the intensities of the mixture lights on the left using either the RGB method or the Lab method (see section 2.5, below).

2.4. Observers

All observers passed the Ishihara color vision test. Forty-six naïve observers were recruited for this experiment, in addition to the 5 experienced observers from our previous paper. Of the new observers, 16 (6 males and 10 females, with an age range of 19 to 29, and an average age of 25 years) made the matches using the RGB method (see next), 26 observers (12 males and 14 females, with an age range of 20 to 31, and an average age of 24.5 years old) made the matches using the Lab method (see next), and four observers (2 males and 2 females, with ages of 21, 29, 28, 30, respectively) made matches using both methods for direct comparison. In addition, the results for 5 male observers are included, who used the RGB method and whose results were reported in our previous paper, with an age range of 21 to 25 years and an average age of 23 years. Among all 51 observers, the age range was 19 to 31 and the average age was 24.3 years.

2.5. Procedure

In this study, two procedures were used to obtain color matches. In the first, the observer matched the reference white by adjusting the intensities of a triplet of lights making up the matching

Optics EXPRESS

mixture half-field. This is called the RGB control method. In the second, the triplet of lights in the mixture half-field were transformed using the GOG model [26] into the CIELAB space and the observer varied the L* (lightness), a* (redness-greenness), b* (yellowness-blueness) to match the reference white. These three dimensions are often presumed to underlie the phenomenology of human color vision, corresponding to opponent color theory of Hering [27]. This is called the Lab control method. Anecdotally, observers found the Lab procedure easier. The reason the Lab method is easier can be explained by considering an example. Imagine the mixture half-field is not red enough. In the RGB method, the R light can be increased to increase redness but this has the unwanted effect of also increasing lightness. Alternatively, the G light can be decreased to increase redness, and this has the effect of decreasing lightness. Consequently, to increase redness but not lightness the observer must adjust the intensities of both the R and G lights. By contrast, in the Lab method redness and lightness can be adjusted approximately independently, which is much more intuitive. However, the Lab method implicitly assumes the observer is close to the CIE standard observer, so may introduce bias in the matches for some non-standard observers and may not be appropriate for observers with color vision deficiency.

A chin rest was used to fix the observer's position at 50 cm from the matching fields, and viewing was binocular. In an otherwise dark room, observers were given brief training on the method for about 15-30 minutes. In the main experiment, after adapting to the testing environment for two minutes, observers made a set of 15 color matches with FOV of 10°. Observers are advised to ignore, if visible, any color difference in the center of the fields (due to Maxwell's spot) and make their matches based on the outer region. After a brief rest and re-adaptation, the observer completed a further set of 15 color matches for the 2° FOV. The 15 settings included two repeats for the four triplets labelled 'standard', 2, 5, and 9 in Table 1 and one for each of the other triplets. The repeated matches were used to estimate intra-observer variability. In total, the experiment took about 90 minutes.

Once the color matches were made, the spectral power distribution (SPDs) of all the triplets that were matched by each observer were measured (from 380 to 780 nm in 1 nm steps) with the spectroradiometer (Konica-Minolta CS2000) positioned in the observer's eye position.

Pupil size and thus retinal illuminance was monitored in these experiments. Typical mean and SD values for the pupil diameter were 2.74 and 0.25 mm, respectively. Thus, there were slight variations in retinal illuminances of the reference and the standard fields due to changes in pupil diameter, but these would not be expected to significantly affect the color matches.

2.6. Derivation of cone spectral sensitivities

The matches for each observer were used to estimate their individual cone spectral sensitivities. As previously mentioned, each observer made 15 matches for both the 2° and 10° FOV (11 matches and 4 repeats for 'standard' triplet and triplets 2, 5, and 9, see Table 1). The repeated matches were used to calculate intra-observer variation. To estimate individual cone spectral sensitivities the repeats were averaged to produce a total of 11 SPDs for each observer's fit.

The analysis assumed that all the matched whites for a given observer and a given FOV should produce the *same* three cone excitations. Consequently, when the SPDs for the matched whites set by a single observer are cross-multiplied with each of his or her three cone spectral sensitivities and summed across wavelength, all the L-cone values should be the same, all the M-cone values should be the same and all the S-cone values should be the same. Our goal in analyzing the color matching data of an observer was to find the three cone spectral sensitivities for that observer for which the three values are most similar. This was achieved by applying the extended CIEPO06 [1] model developed by Stockman and Rider [28], in which the L-, M- and S-cone absorbance spectra and the standard lens and macular optical density spectra are defined as continuous functions of wavelength, and are then parametrically combined to produce corneal spectral sensitivities.

Optics EXPRESS

Here the seven parameters of the model - the optical densities of the L-, M- and S-cones (l_{OD}, m_{OD} and s_{OD}) the lens and macular densities (k_{lens} and k_{mac}), and the spectral shifts of the L and M cones (L_{shift} and M_{shift}) - were optimized to minimize the squared differences in the L, M and S-cone excitations across the 11 matched white spectra (the 4 repeats are averaged). For full detail of the model functions and parameters please refer to Stockman and Rider [28].

The model was fitted simultaneously to all the 2° and 10° matched white SPDs for a single observer (22 matches) using Matlab's GlobalSearch procedure. A total of 11 parameters for each individual was fitted. The CIEPO06 model explicitly assumes that three parameters are constant across FOV (L_{shift}, M_{shift} and k_{lens}), while the other four parameters (k_{mac}, l_{OD}, m_{OD} and s_{OD}) vary with FOV.

3. Results

3.1. Intra- and inter-observer variability for the RGB and lab color matches

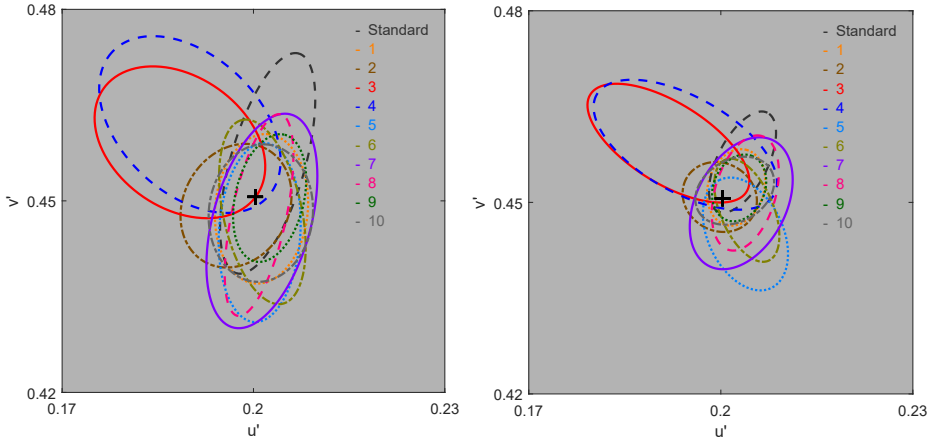

Fig. 2. The 95% confidence ellipses for each primary set in the 2° experiment (left: RGB control method, right: Lab control method, '+': reference white).

Intra- and inter-observer variations of the RGB and Lab control methods were calculated using the CIE 2000 color-difference formula, in ΔE_{00} units [29]. Figure 2 plots the 95% confidence ellipses for each of the triplets used in the 2° experiment in the u', v' co-ordinates underlying CIE 1976 LUV color space. Note, this color space was used as it is closer to a "perceptually uniform" color space than LMS, RGB or XYZ. We calculated the coordinates by first converting the SPD of the matches into LMS values using the standard CIEPO06 observer, and then transforming these to u', v' coordinates. The RGB control method results are plotted in the left-hand panel and have average intra- and inter-observer variabilities of 2.53 and 5.77 ΔE_{00}, respectively (the mean SDs are 0.91 and 2.11 ΔE_{00}, respectively). The Lab control method results are plotted in the righthand panel and have average intra- and inter-observer variabilities of 1.14 and 2.62 ΔE_{00} units (the mean SDs are 0.31 and 0.96 ΔE_{00}), respectively. Under the Lab method both intra- and inter-observer variabilities were less than half that under the RGB method. The ellipses obtained using the two methods are clearly different in shape and size, perhaps reflecting the different linkages between perceptual color space and the physical controls. For example, the strong correlation between brightness and redness-greenness in the RGB method might make it harder to adjust the lights to find the perfect match. However, the ellipse centers are generally consistent, the mean color difference between the centers of the ellipses in the two methods was 2.88 in ΔE_{00} units (1.20 ΔE_{00} of SD). The mean matching errors (distance from the reference white,

Optics EXPRESS

shown the black cross, to the center of the ellipses) were 7.68 and 7.33 ΔE_{00} for the RGB and Lab method (the mean SDs are 4.37 and 4.02 ΔE_{00}), respectively. These values are consistent with the values from our previous study with experienced observers where the mean matching error for 2° matches was 7.72 ΔE_{00}. This is encouraging as the experienced observers made a more comprehensive set of measurements – a total of 55 matches per FOV, rather than the reduced number of matches made in this experiment. It is also worth noting that the reference light (black cross) plots to a point within most of the ellipses in Figs. 2 and 3, indicating that the standard observer model can be considered a reasonable approximation for these "color normal" observers. Below we examine whether and how much our individualized model provides a better fit.

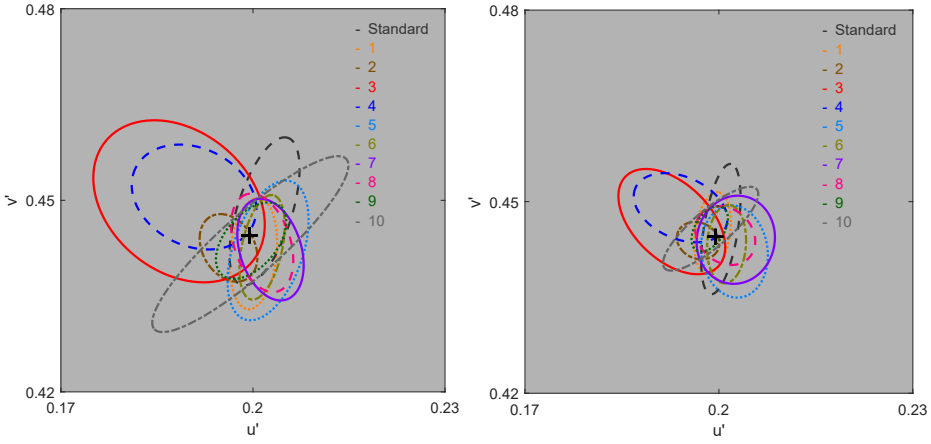

Fig. 3. The 95% confidence ellipses for each primary set in the 10° experiment (left: RGB control method, right: Lab control method, '+': reference white).

Similar results were obtained in the 10° FOV experiment. For the RGB control method, intra-, inter-observer variability were 1.06 and 4.15 ΔE_{00} (the mean SDs are 0.36 and 1.71 ΔE_{00}), respectively, and the mean matching error was 5.50 ΔE_{00} (3.08 ΔE_{00} of SD). For the Lab method, intra-, inter-observer variability were 0.64 and 1.93 ΔE_{00}(the mean SDs are 0.16 and 0.67 ΔE_{00}), respectively, and the mean matching error was 4.19 ΔE_{00} (1.51 ΔE_{00} of SD). The matching errors are again consistent with the experienced observers in our previous experiment, 5.09 ΔE_{00}. Figure 3 shows the 95% confidence ellipses of the 10° experiments with different control methods. Again, the Lab method gives lower variability and slightly better matching errors, but again the centers are consistent, the mean color difference between the centres of the ellipses in the two methods was 2.61 in ΔE_{00} units (1.12 ΔE_{00} of SD), which is much smaller than the inter-observer matching errors.

As a control, four observers carried out matches using both the RGB and the Lab control methods. The variability as expected was greater using the RGB method, but both methods yielded consistent estimates of the underlying individual differences. Conservatively, we class significant differences as those that are more than twice the standard deviation. No parameter estimates met this threshold. The Lab method was therefore intuitively easier for the observers but did not alter the results of the analysis. Tables 11 and 12 in the Appendix for 2° and 10° FOV, respectively, give the individual parameter fits for the 4 observers who used both methods.

3.2. *Derivation of individual cone spectral sensitivities*

As outlined in Section 2.5, we fitted the model by adjusting the optical densities of the L-, M- and S-cones (l_{OD}, m_{OD} and s_{OD}), the lens and macular densities (k_{lens} and k_{mac}), and the spectral shifts of the L- and M-cones (L_{shift} and M_{shift} in nm) to minimise the least squared error in the

Optics EXPRESS

L-, M- and S-cone excitations across the 22 matches for each observer. The model was fitted simultaneously to all the 2° and 10° FOV matches, it being assumed that three parameters (L_{shift}, M_{shift} and k_{lens}) are the same for the 2° and 10° FOV. The fits for each individual observer are tabulated in Tables 7–10 in the Appendix. Table 2 summarizes the mean fits.

Table 2. Summary of the means and standard deviations of the best-fitting parameters for the RGB and Lab methods and for both methods combined. The parameter lens gives the density of the lens pigment at 400 nm and mac the optical density of macular pigment at 460 nm. The yellow highlights show those parameters that are > 2 SD away from the CIE standard values.

FOV	Method		L_{shift}	M_{shift}	l_{OD}	m_{OD}	s_{OD}	k_{lens}	k_{mac}
2°	RGB (n = 21)	Mean	-0.76	2.88	0.50	0.44	0.37	1.74	0.402
		SD	1.36	1.32	0.09	0.10	0.03	0.20	0.040
	Lab (n = 30)	Mean	0.26	2.66	0.48	0.48	0.36	1.84	0.426
		SD	0.82	1.23	0.08	0.09	0.03	0.18	0.032
	Mean of all (n = 51)	Mean	-0.25	2.77	0.49	0.46	0.37	1.79	0.414
		SD	1.09	1.28	0.09	0.10	0.03	0.19	0.036
	CIE	PO06	0	0	0.50	0.50	0.40	1.76	0.35
10°	RGB (n = 21)	Mean	-0.76	2.88	0.44	0.42	0.32	1.74	0.101
		SD	1.36	1.32	0.06	0.09	0.04	0.20	0.013
	Lab (n = 30)	Mean	0.26	2.66	0.43	0.42	0.29	1.84	0.096
		SD	0.82	1.23	0.07	0.08	0.04	0.18	0.011
	Mean of all (n = 51)	Mean	-0.25	2.77	0.44	0.42	0.31	1.79	0.098
		STD	1.09	1.28	0.07	0.09	0.04	0.19	0.011
	CIE	PO06	0	0	0.38	0.38	0.30	1.76	0.095

Separate analyses of the data for male and female observers showed no systematic or statistically significant differences. That is, no parameters differed between sexes by as much as two standard deviations.

The best-fitting parameters for each observer are plotted in Fig. 4 for the 2° FOV and in Fig. 5 for the 10° FOV. In both figures, the fitted parameters are shown as blue and red circles for the RGB and Lab methods, respectively. The means and ± 1SD are shown by the solid and dashed lines, respectively in the corresponding colors. The CIEPO06 standard values are shown by the solid white lines. Since the L-shift, M-shift, and lens parameters are the same for 2° and 10° they are only plotted in Fig. 4.

The parameters obtained with the RGB and Lab methods overlap and are not significantly different. Thus, it can be concluded that even though one method produces more variability in the match settings, the resulting estimates of the underlying individual differences are essentially unaffected and show no systematic differences. Therefore, the above is justified in combining the results across the methods.

The parameters also do not differ significantly from the parameters assumed in the CIEPO06 model (i.e., they are less than 2SD different) with two exceptions. First, and of some interest, is that the M-cone photopigment is shifted by about 3 nm to longer wavelengths. Second, the macular estimate for 2° is slightly denser but only significantly so for the Lab method.

3.3. Parameter variance and covariance

With model fitting of this type, it is relatively straightforward to obtain best fitting parameter values using numerical optimization methods, but it is difficult to extract reliable measures

Optics EXPRESS

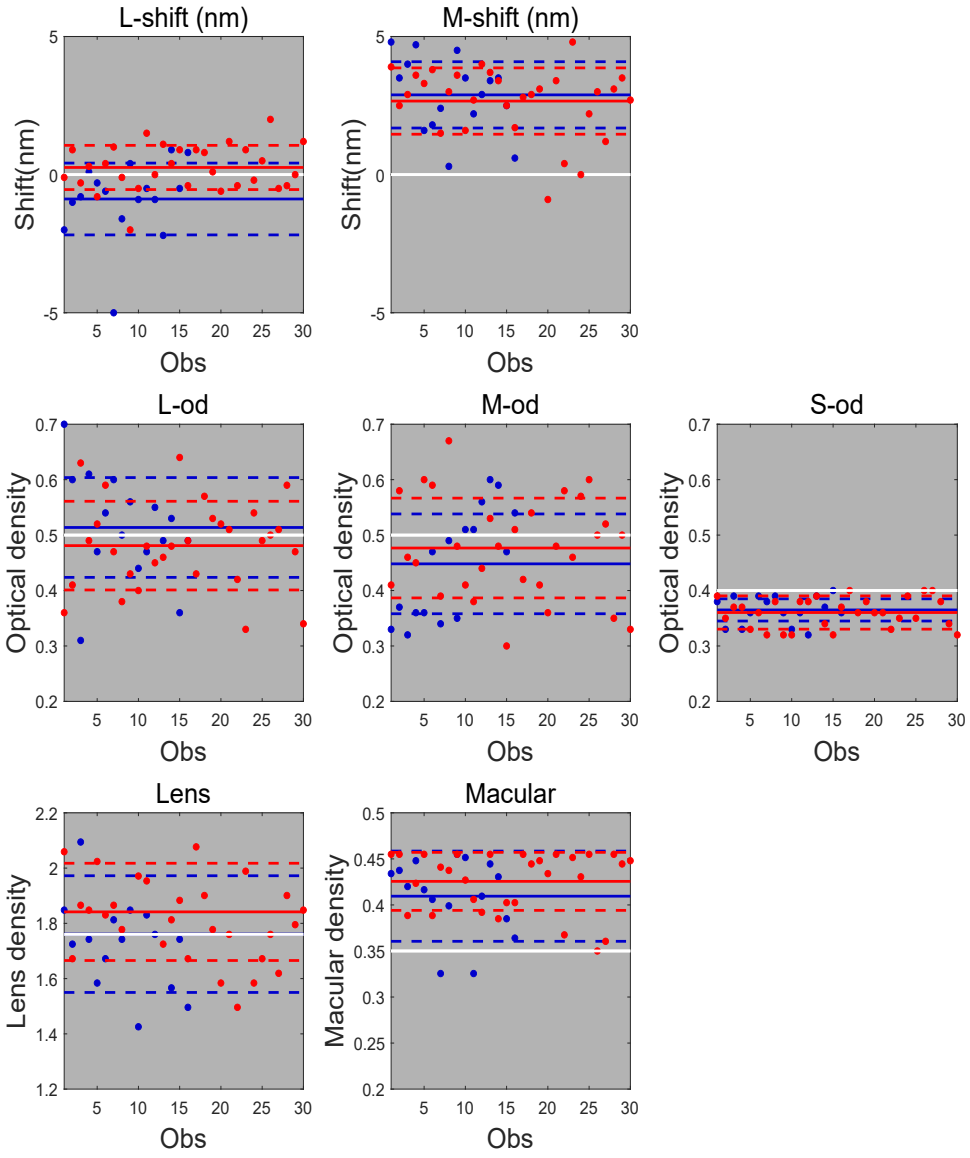

Fig. 4. The distribution of 2° fitted parameters for the RGB method (blue circles) and the Lab method (red circles). The RGB means are shown by the solid blue lines and ± 1SD by the blue dashed lines. The Lab means are shown by the solid red lines and ± 1SD by the red dashed lines. The CIEPO06 assumptions are shown by the solid white lines. Note that the L-shift, M-shift, and lens parameters are the same for 2 and 10°.

of the uncertainty of those parameters. An important issue is not only the variability of the parameters, but how different parameters in the fit covary. To explore the differences between individual observers and the variability and correlation in the fitted parameters, a bootstrapping method for data resampling and refitting was employed. In brief, for each observer's 11 sets of matching data under a specific field of view, random sampling with replacement to form a "new" set of matches for that field of view was used, and applied our model to the 22 bootstrapped samples (simultaneously fitting both FOVs, as above) to gain a new set of parameter estimates.

Optics EXPRESS

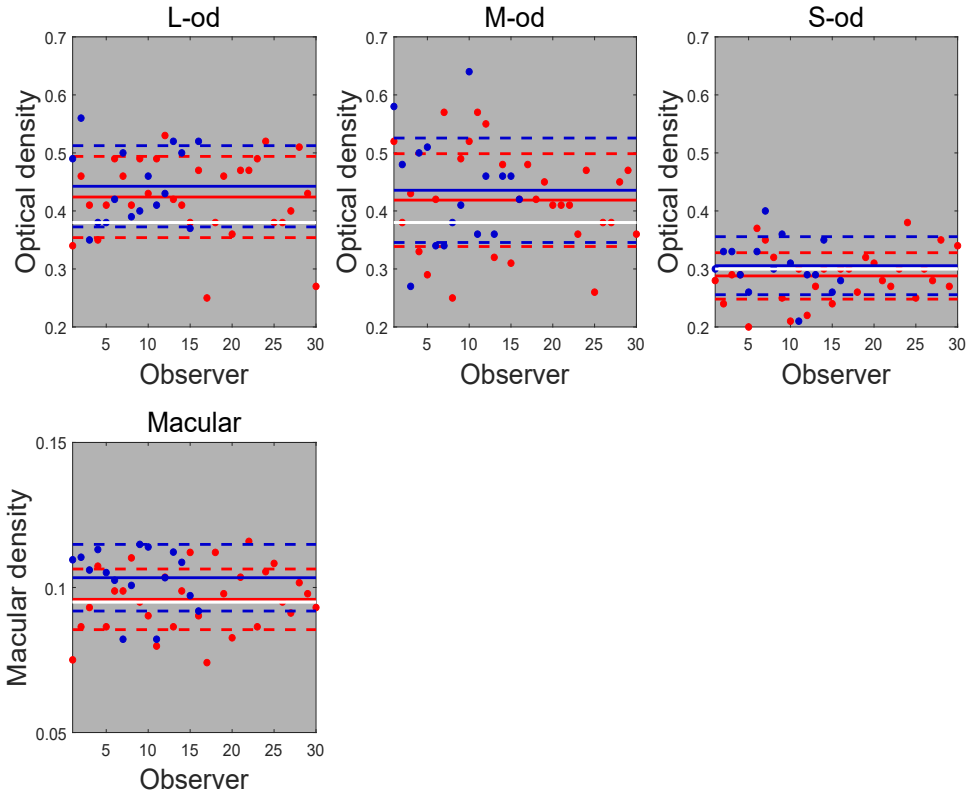

Fig. 5. The distribution of 10° fitted parameters, means and SD. Details as for Fig. 4. The L-shift, M-shift, and lens parameters are not shown since they are the same as in Fig. 4.

This process was repeated 1000 times to get a bootstrapped parameter population. From these individual observers mean and standard deviations of the parameter values were calculated as well as correlation matrices between the fitted parameters and then averaged these across observers separately for the RGB or Lab methods to give overall measures of uncertainty across all the fits. The bootstrapped means and average standard deviations are given in Table 3 and 4. The means are close to the population means in Tables 7–10 of the Appendix, while the standard deviations are smaller than the population standard deviations meaning there is lower variability in the fits than across the observers.

Table 3. Summary of the average parameter values and standard deviations from bootstrapped analysis of the RGB and Lab methods for the 2° FOV.

Method		L_{shift}	M_{shift}	l_{OD}	m_{OD}	s_{OD}	k_{lens}	k_{mac}
RGB	Mean	-0.7248	2.7741	0.5046	0.4519	0.3640	1.7489	0.4065
	Average bootstrap SD	0.6471	0.7821	0.0286	0.0269	0.0187	0.0583	0.0110
Lab	Mean	0.2673	2.4530	0.4815	0.4869	0.3530	1.8477	0.4219
	Average bootstrap SD	0.5794	0.6204	0.0274	0.0258	0.0147	0.0599	0.0076

Correlation matrices are given in Tables 5 and 6. the highlighted are the strongly correlated parameters ($|r| > 0.6$) in red. Interestingly, there are stronger correlations for the Lab method

Optics EXPRESS

than for the RGB. We do not know why this is the case, but the overall variability of the fits in the RGB method to be slightly higher, particularly for the L and M-cone shifts, than those in the Lab method (see Tables 3 and 4), and this will reduce the correlation slightly. The strongest correlations are in the same directions for both methods and no significant correlations were found that were positive for one method and negative for the other. Importantly, all of the strongest correlations are between the spectral shifts and optical densities of the L- and M-cones, and the lens density. This makes intuitive sense as the lens selectively blocks shorter-wavelength light, so increasing the lens density would primarily reduce the overall sensitivity of the S-cones (note, our model has no parameters for overall sensitivity, it is the spectral shape that is important), and would spectrally skew the sensitivity of L- and M-cones, causing an apparent shift to longer wavelengths and a narrower spectral profile. The model can therefore trade off lens density against spectral shifts with compensatory changes of cone optical density to adjust the spectral bandwidth of the L- and M-cones. The macular and S-cone optical densities were not strongly correlated with each other nor with any other parameters, suggesting the S-cone spectral sensitivity can be estimated independently of the L- and M-cones. Although there are some high correlations between some of the other parameters of the model, it is worth noting that the variability in the fitted parameters is relatively low (Tables 3 and 4), so the overall fits are well constrained. Also, as noted above, the highest correlations are among lens and L- and M-cone parameters, and these correlated such that they are likely to arrive at similarly shaped cone spectral sensitivities.

Table 4. Summary of the average parameter values and standard deviations from bootstrapped analysis of the RGB and lab methods for the 10° FOV.

Method		L_{shift}	M_{shift}	l_{OD}	m_{OD}	s_{OD}	k_{lens}	k_{mac}
RGB	Mean	-0.7248	2.7741	0.4406	0.4410	0.3024	1.7489	0.1062
	Average bootstrap SD	0.6471	0.7821	0.0344	0.0261	0.0136	0.0583	0.0036
Lab	Mean	0.2673	2.4530	0.4343	0.4226	0.2983	1.8477	0.0962
	Average bootstrap SD	0.5794	0.6204	0.0280	0.0262	0.0129	0.0599	0.0031

Table 5. Summary of the correlation matrices derived via bootstrapping from the RGB method for combined 2° and 10° FOV fits. Strong correlations ($|r| > 0.6$) are highlighted in red. Correlations of opposite sign to those in Table 6 are highlighted in blue.

RGB method	L_{shift}	M_{shift}	l_{OD} 2°	m_{OD} 2°	s_{OD} 2°	k_{lens}	k_{mac} 2°	l_{OD} 10°	m_{OD} 10°	s_{OD} 10°	k_{mac} 10°
L_{shift}	-	-0.02	-0.32	-0.59	-0.03	-0.24	0.18	-0.33	-0.66	-0.18	0.05
M_{shift}	-0.02	-	-0.71	-0.35	0.19	-0.63	-0.23	-0.81	-0.15	-0.04	-0.26
l_{OD} 2°	-0.32	-0.71	-	0.30	0.03	0.50	-0.01	0.75	0.29	0.18	0.15
m_{OD} 2°	-0.59	-0.35	0.30	-	-0.17	0.34	-0.01	0.53	0.65	0.07	0.03
s_{OD} 2°	-0.03	0.19	0.03	-0.17	-	-0.12	0.02	-0.20	-0.29	0.08	-0.06
k_{lens}	-0.24	-0.63	0.50	0.34	-0.12	-	0.13	0.51	0.23	-0.17	0.05
k_{mac} 2°	0.18	-0.23	-0.01	-0.01	0.02	0.13	-	0.11	-0.22	-0.07	0.07
l_{OD} 10°	-0.33	-0.81	0.75	0.53	-0.20	0.51	0.11	-	0.46	0.19	0.13
m_{OD} 10°	-0.66	-0.15	0.29	0.65	-0.29	0.23	-0.22	0.46	-	0.09	0.04
s_{OD} 10°	-0.18	-0.04	0.18	0.07	0.08	-0.17	-0.07	0.19	0.09	-	-0.02
k_{mac} 10°	0.05	-0.26	0.15	0.03	-0.06	0.05	0.07	0.13	0.04	-0.02	-

Optics EXPRESS

Table 6. Summary of the correlation matrices derived via bootstrapping from the lab method for combined 2° and 10° FOV fits. Strong correlations (|r| > 0.6) are highlighted in red.

Lab method	L_{shift}	M_{shift}	l_{OD} 2°	m_{OD} 2°	s_{OD} 2°	k_{lens}	k_{mac} 2°	l_{OD} 10°	m_{OD} 10°	s_{OD} 10°	k_{mac} 10°
L_{shift}	-	-0.15	-0.52	-0.73	0.10	-0.38	0.30	-0.55	-0.85	-0.23	0.09
M_{shift}	-0.15	-	-0.78	-0.52	0.47	-0.82	-0.20	-0.85	-0.42	0.13	-0.29
l_{OD} 2°	-0.52	-0.78	-	0.54	-0.19	0.70	-0.01	0.85	0.60	-0.04	0.19
m_{OD} 2°	-0.73	-0.52	0.54	-	-0.42	0.60	-0.19	0.77	0.84	0.29	0.04
s_{OD} 2°	0.10	0.47	-0.19	-0.42	-	-0.54	0.07	-0.44	-0.37	-0.11	-0.11
k_{lens}	-0.38	-0.81	0.69	0.60	-0.54	-	0.06	0.74	0.55	-0.28	0.08
k_{mac} 2°	0.30	-0.19	-0.01	-0.19	0.07	0.06	-	-0.05	-0.37	-0.46	0.09
l_{OD} 10°	-0.55	-0.84	0.85	0.77	-0.43	0.74	-0.05	-	0.75	0.18	0.12
m_{OD} 10°	-0.85	-0.41	0.60	0.84	-0.37	0.55	-0.37	0.75	-	0.35	0.10
s_{OD} 10°	-0.23	0.12	-0.04	0.29	-0.11	-0.28	-0.46	0.18	0.35	-	-0.13
k_{mac} 10°	0.09	-0.29	0.19	0.04	-0.10	0.08	0.09	0.12	0.10	-0.13	-

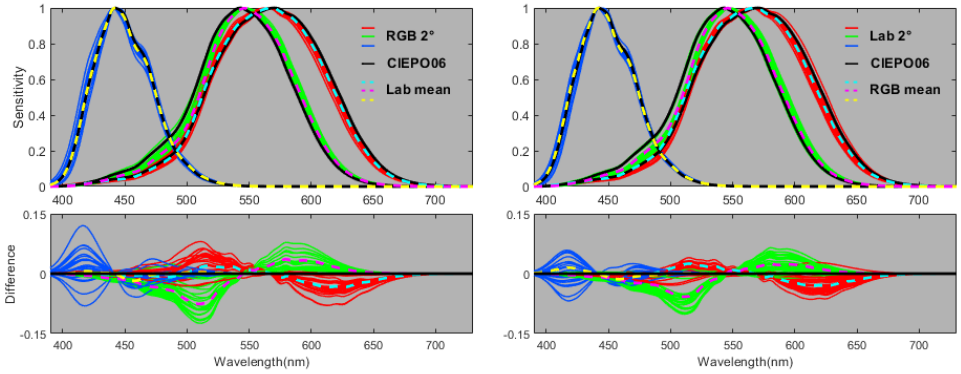

Fig. 6. 2° cone fundamentals. Upper left: Individualized cone fundamentals estimated for 25 observers using the RGB method (20 in this study and 5 replotted from Shi et al [17]). Red, green and blue curves denote L-, M- and S-cone fundamentals, respectively. Solid black curves denote CIEPO06 2° cone fundamentals. Dashed cyan, magenta, and yellow curves denote the mean of the L-, M- and S-cone fundamentals derived with the Lab method. Upper right: Estimated cone fundamentals for our 30 observers using the Lab method. Red, green, and blue curves denote L-, M- and S-cone fundamentals, respectively. Solid black curves denote CIEPO06 2° cone fundamentals. Dashed cyan, magenta, and yellow curves denote the mean of the L-, M- and S-cone fundamentals derived with the RGB method. Lower left: Differences between the CIEPO06 2° cone fundamentals and the individual functions estimated with RGB method. Figure conventions as in upper left panel. Lower right: Differences between the CIEPO06 2° cone fundamentals and the individual functions estimated with Lab method. Figure conventions as in upper right panel.

Optics EXPRESS

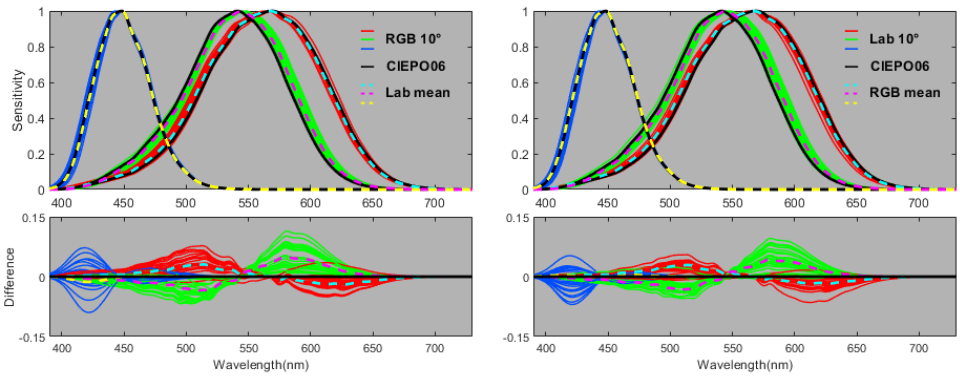

Fig. 7. 10° cone fundamentals. Details as for Fig. 6 but for the 10° matches and data and for the CIEPO06 10° cone fundamentals.

3.4. Cone spectral sensitivities

All 51 individual fitted cone fundamentals for 2° and 10° FOV are shown in Figs. 6 and 7, respectively. The top left panels show the L-, M- and S-cone fundamentals estimated under the RGB control method (as red, green and blue curves, respectively). For comparison, the black curves are CIEPO06 (2° or 10° standard, in Fig. 6 or 7, respectively) standard cone fundamentals and the mean L-, M- and S-cone fundamentals estimated under the Lab control method are shown as the cyan, magenta and yellow dashed curves, respectively. Lower panels show the difference between the individually fitted cone fundamentals and the CIEPO06 standard.

As expected from Table 2 and Figs. 4 and 5, the M-cone fundamentals estimated using the RGB and Lab methods both show a small shift towards longer wavelengths compared to CIEPO06 M-cone fundamental, i.e., relative to the CIEPO06 standard, our model consistently shows reduced M-cone sensitivity below about 550 nm and increased sensitivity above 550 nm. There is also a suggestion that for many of our observers the L-cone fundamentals estimated using either the RGB or Lab methods show a smaller shift in the opposite direction towards shorter wavelengths. The differences between the fundamentals obtained using the RGB and Lab methods are small.

4. Discussion and conclusions

Human color vision varies between observers because of individual differences in macular and lens optical densities, photopigment optical densities and genetically determined spectral shifts in the cone absorbance spectra. In this study, a set of color matching experiments was conducted using Maxwell's method from which the individual L-, M- and S-cone spectral sensitivities were estimated. The resulting spectral sensitivities are largely consistent with the CIEPO06 standard observer, which some small deviations, see below. This is encouraging as our observers all had normal color vision (probably, see below) and were of a similar age to those whose data informed the CIEPO06 standard. Age is known to affect the optical density of the lens in particular, which selectively blocks shortwave light and will therefore affect color matches. We are currently extending our study to include a broader range of ages to examine these effects in our model.

Optics EXPRESS

In our study the criterion for inclusion as a color normal observer was to pass the Ishihara color test. The test is useful for identifying observers who are dichromats (having only either an L- or an M-cone photopigment gene) and those with moderate to severely anomalous trichromacy (whose L and or M-cone photopigment gene(s) are different from normal, but produce spectral sensitivities that are distinct enough to produce some red-green color vision). Some observers with mild anomalous trichromacy might pass the Ishihara test, but their anomaly should be apparent in our measurements and from our analysis. We are currently recruiting mild to severely anomalous trichromats to perform our color matching experiment and in a future study will examine whether the method and model can be useful in determining the spectral shift of their hybrid opsin.

The mean spectral shift of the M-cone cone spectral sensitivity was approximately 3 nm and is the largest apparent deviation in our findings from the CIEPO06 standard observer model. While this size of shift is consistent with a hybrid M-cone opsin gene with either serine replacing alanine at codon 180 in exon 3 or isoleucine replacing threonine at codon 230 in exon 4 [30], we are unaware of any evidence that these polymorphisms are more prevalent among the Chinese population from which we recruited our observers compared to the Western populations that were included in the CIE standards. For example, Winderickx *et al.* [31] in a sample of 75 color normal Caucasians found none had isoleucine at codon 230 on their M-cone gene and just 6% had serine at codon 180. Further genetic analysis of these populations would be extremely useful in confirming or refuting a hybrid gene hypothesis. Also relevant is the fact that the genotyped dichromat observers who contributed data to produce the Stockman and Sharpe cone fundamentals (i.e., the CIEPO06 standard) were all male single-gene dichromats known to have either wildtype M opsin or L with serine at amino acid position 180 [32,33] meaning their L- and M-cone spectral positions were located at the extremes of the general population. Thus, the CIEPO06 spectral sensitivities do not include polymorphic variants that might shift the M-cone photopigment to slightly longer wavelengths and the L-cone pigment to slightly shorter wavelengths. The shifts we find in the observers in our study might reflect polymorphic variants in our population. Furthermore, our observers included a slight majority of females (52%) with the potential not only of hybrid L- or M-cone opsin genes, but also of different polymorphisms on their two X chromosomes [34]. While this could potentially lead to tetrachromacy, the evidence for functional tetrachromacy is weak [35] and it would most likely produce mixed cone fundamentals that are effectively intermediate between the two genes. However, it was found that no significant difference in either the L or M-cone shifts between males and females.

In conclusion, color matching experiments were carried out with a large cohort of young color normal observers and used these data and a parametric physiological model of spectral sensitivity to estimate individual cone fundamentals and the causes of the individual differences. The results are encouragingly consistent with the CIEPO06 standards, with the main exception of a small shift in M-cone spectral sensitivity to longer wavelengths. Work is ongoing to apply these same methods to other groups whose cone fundamentals are likely to deviate more significantly from the standard observer, such as older observers and observers with color vision deficiencies.

Optics EXPRESS

Appendix: model fits and estimates of uncertainty

Table 7. The 2° parameters for the 21 young observers using RGB method (The first 5 are the observers from our previous paper, and the last 16 are the participants in the experiment of this paper).

Observer	Gender	Age	L_{shift}	M_{shift}	l_{OD}	m_{OD}	s_{OD}	*lens* (At 400 nm)	*macular* (At 460 nm)	Fitting error (%)
A1	M	22	-1.20	2.10	0.49	0.43	0.36	1.55	0.370	1.75
A2	M	25	0.20	2.90	0.47	0.36	0.38	1.90	0.384	1.49
A3	M	21	-0.60	3.50	0.49	0.42	0.42	1.67	0.379	2.44
A4	M	22	0.20	3.30	0.45	0.41	0.35	1.67	0.373	1.97
A5	M	24	-0.50	2.50	0.47	0.43	0.35	1.64	0.381	1.19
RGB1	F	26	-2.00	4.80	0.70	0.33	0.38	1.85	0.433	2.37
RGB2	M	27	-1.00	3.50	0.60	0.37	0.33	1.72	0.439	2.43
RGB3	F	23	-0.80	4.00	0.31	0.32	0.39	2.10	0.419	1.89
RGB4	F	24	0.10	4.70	0.61	0.36	0.33	1.73	0.447	2.47
RGB5	F	25	-0.30	1.60	0.47	0.36	0.36	1.59	0.415	2.38
RGB6	F	29	-0.60	1.80	0.54	0.47	0.39	1.68	0.405	1.98
RGB7	F	24	-5.00	2.40	0.60	0.34	0.38	1.81	0.326	2.66
RGB8	F	24	-1.60	0.30	0.50	0.49	0.39	1.74	0.400	1.72
RGB9	F	19	0.40	4.50	0.56	0.35	0.36	1.84	0.454	2.89
RGB10	M	22	-0.90	3.50	0.44	0.51	0.33	1.43	0.452	2.25
RGB11	M	26	-0.50	2.20	0.47	0.51	0.36	1.82	0.324	1.58
RGB12	F	26	-0.90	2.90	0.55	0.56	0.32	1.76	0.410	2.20
RGB13	F	24	-2.20	3.40	0.49	0.60	0.39	2.29	0.445	3.09
RGB14	M	21	0.90	3.50	0.53	0.59	0.37	1.57	0.430	1.59
RGB15	M	26	-0.50	2.50	0.36	0.47	0.40	1.75	0.384	2.51
RGB16	M	26	0.80	0.60	0.49	0.54	0.36	1.49	0.365	1.50
Mean		24.41	-0.76	2.88	0.50	0.44	0.37	1.74	0.402	2.25
STD		2.37	1.36	1.32	0.09	0.10	0.03	0.20	0.040	
CIEPO06 standard vlaues			0.00	0.00	0.50	0.50	0.40	1.76	0.350	

Optics EXPRESS

Table 8. The 2° parameters for the 30 young observers using lab method.

Observer	Gender	Age	L_{shift}	M_{shift}	l_{OD}	m_{OD}	s_{OD}	*lens* (At 400 nm)	*macular* (At 460 nm)	Fitting error (%)
LAB1	M	20	-0.10	3.90	0.36	0.41	0.39	2.06	0.455	1.96
LAB2	F	21	0.90	2.50	0.41	0.58	0.35	1.67	0.455	2.18
LAB3	F	24	-0.30	2.90	0.63	0.46	0.37	1.87	0.389	2.01
LAB4	F	21	0.30	3.60	0.49	0.45	0.37	1.84	0.423	1.56
LAB5	M	24	-0.80	3.30	0.52	0.60	0.33	2.02	0.455	2.04
LAB6	F	29	0.40	3.80	0.59	0.59	0.36	1.83	0.389	2.00
LAB7	F	24	1.00	1.50	0.47	0.39	0.32	1.86	0.440	1.97
LAB8	M	28	-0.10	3.00	0.38	0.67	0.38	1.77	0.437	1.64
LAB9	M	25	-2.00	3.60	0.43	0.48	0.32	2.27	0.453	2.20
LAB10	M	30	-0.50	1.60	0.40	0.41	0.32	1.97	0.428	1.42
LAB11	M	25	1.50	2.70	0.48	0.38	0.38	1.95	0.406	1.89
LAB12	F	24	0.00	4.00	0.45	0.44	0.38	2.26	0.393	2.38
LAB13	F	31	1.10	3.70	0.46	0.53	0.39	1.73	0.455	1.86
LAB14	M	22	0.40	3.40	0.48	0.48	0.34	1.81	0.386	1.30
LAB15	F	23	0.90	2.50	0.64	0.30	0.32	1.87	0.402	1.82
LAB16	M	27	-0.40	1.70	0.49	0.51	0.37	1.67	0.401	1.78
LAB17	F	26	0.90	2.80	0.43	0.42	0.40	2.07	0.455	2.55
LAB18	M	26	0.80	2.90	0.57	0.54	0.36	1.90	0.444	1.31
LAB19	F	23	0.10	3.10	0.53	0.41	0.38	1.78	0.450	2.08
LAB20	F	26	-0.60	-0.90	0.52	0.36	0.36	1.58	0.433	1.24
LAB21	M	23	1.20	3.40	0.51	0.48	0.36	1.76	0.455	1.60
LAB22	F	27	-0.40	0.40	0.42	0.58	0.33	1.49	0.367	0.86
LAB23	F	26	0.90	4.80	0.33	0.46	0.35	1.99	0.453	2.16
LAB24	M	21	-0.20	0.00	0.54	0.57	0.39	1.59	0.432	0.83
LAB25	M	26	0.50	2.20	0.49	0.60	0.35	1.67	0.455	1.67
LAB26	M	23	2.00	3.00	0.50	0.50	0.40	1.76	0.350	2.94
LAB27	M	28	-0.50	1.20	0.51	0.52	0.40	1.62	0.362	2.00
LAB28	F	26	-0.40	3.10	0.59	0.35	0.38	1.91	0.454	1.56
LAB29	F	22	0.00	3.50	0.47	0.50	0.34	1.79	0.444	2.02
LAB30	F	28	1.20	2.70	0.34	0.33	0.32	1.85	0.447	1.62
Mean		24.97	0.26	2.66	0.48	0.48	0.36	1.84	0.426	1.81
STD		2.76	0.82	1.23	0.08	0.09	0.03	0.18	0.032	
CIEPO06 standard vlaues			0.00	0.00	0.38	0.38	0.30	1.76	0.095	

Optics EXPRESS

Table 9. The 10° parameters for the 21 young observers using RGB method. (The first 5 are the observers from our previous paper, and the last 16 are the participants in the experiment of this paper.)

Observer	Gender	Age	L_{shift}	M_{shift}	l_{OD}	m_{OD}	s_{OD}	*lens* (At 400 nm)	*macular* (At 460 nm)	Fitting error (%)
A1	M	22	-1.20	2.10	0.46	0.37	0.40	1.55	0.107	1.14
A2	M	25	0.20	2.90	0.43	0.31	0.41	1.90	0.116	1.16
A3	M	21	-0.60	3.50	0.47	0.36	0.40	1.67	0.107	1.36
A4	M	22	0.20	3.30	0.43	0.35	0.39	1.67	0.105	1.13
A5	M	24	-0.50	2.50	0.47	0.37	0.33	1.64	0.106	0.88
RGB1	F	26	-2.00	4.80	0.49	0.58	0.30	1.85	0.090	1.37
RGB2	M	27	-1.00	3.50	0.56	0.48	0.33	1.72	0.080	1.01
RGB3	F	23	-0.80	4.00	0.35	0.27	0.33	2.10	0.118	0.99
RGB4	F	24	0.10	4.70	0.38	0.50	0.29	1.73	0.079	1.03
RGB5	F	25	-0.30	1.60	0.38	0.51	0.26	1.59	0.107	1.68
RGB6	F	29	-0.60	1.80	0.42	0.34	0.33	1.68	0.090	0.80
RGB7	F	24	-5.00	2.40	0.50	0.34	0.40	1.81	0.085	2.10
RGB8	F	24	-1.60	0.30	0.39	0.38	0.30	1.74	0.084	1.42
RGB9	F	19	0.40	4.50	0.40	0.41	0.36	1.84	0.097	1.75
RGB10	M	22	-0.90	3.50	0.46	0.64	0.31	1.43	0.093	1.36
RGB11	M	26	-0.50	2.20	0.41	0.36	0.21	1.82	0.113	1.11
RGB12	F	26	-0.90	2.90	0.43	0.46	0.29	1.76	0.121	0.61
RGB13	F	24	-2.20	3.40	0.52	0.36	0.29	2.29	0.110	1.59
RGB14	M	21	0.90	3.50	0.50	0.46	0.35	1.57	0.115	0.78
RGB15	M	26	-0.50	2.50	0.37	0.46	0.26	1.75	0.103	1.23
RGB16	M	26	0.80	0.60	0.52	0.42	0.28	1.49	0.099	0.71
Mean		24.41	-0.76	2.88	0.44	0.42	0.32	1.74	0.101	1.29
STD		2.37	1.36	1.32	0.06	0.09	0.04	0.20	0.013	
CIEPO06 standard			0.00	0.00	0.50	0.50	0.40	1.76	0.350	

Optics EXPRESS

Table 10. The 10° parameters for the 30 young observers using lab method.

Observer	Gender	Age	L_{shift}	M_{shift}	l_{OD}	m_{OD}	s_{OD}	*lens* (At 400 nm)	*macular* (At 460 nm)	Fitting error (%)
LAB1	M	20	-0.10	3.90	0.34	0.52	0.28	2.06	0.075	1.14
LAB2	F	21	0.90	2.50	0.46	0.38	0.24	1.67	0.086	1.35
LAB3	F	24	-0.30	2.90	0.41	0.43	0.29	1.87	0.094	0.84
LAB4	F	21	0.30	3.60	0.35	0.33	0.29	1.84	0.107	0.82
LAB5	M	24	-0.80	3.30	0.41	0.29	0.20	2.02	0.086	0.85
LAB6	F	29	0.40	3.80	0.49	0.42	0.37	1.83	0.098	0.94
LAB7	F	24	1.00	1.50	0.46	0.57	0.35	1.86	0.099	1.39
LAB8	M	28	-0.10	3.00	0.41	0.25	0.32	1.77	0.110	0.66
LAB9	M	25	-2.00	3.60	0.49	0.49	0.25	2.27	0.095	1.74
LAB10	M	30	-0.50	1.60	0.43	0.52	0.21	1.97	0.090	1.17
LAB11	M	25	1.50	2.70	0.49	0.57	0.30	1.95	0.080	1.86
LAB12	F	24	0.00	4.00	0.53	0.55	0.22	2.26	0.103	1.44
LAB13	F	31	1.10	3.70	0.42	0.32	0.27	1.73	0.087	1.13
LAB14	M	22	0.40	3.40	0.41	0.48	0.30	1.81	0.099	0.91
LAB15	F	23	0.90	2.50	0.38	0.31	0.24	1.87	0.112	0.50
LAB16	M	27	-0.40	1.70	0.47	0.42	0.30	1.67	0.090	1.10
LAB17	F	26	0.90	2.80	0.25	0.48	0.30	2.07	0.074	1.32
LAB18	M	26	0.80	2.90	0.38	0.42	0.26	1.90	0.112	0.64
LAB19	F	23	0.10	3.10	0.46	0.45	0.32	1.78	0.098	1.02
LAB20	F	26	-0.60	-0.90	0.36	0.41	0.31	1.58	0.083	0.59
LAB21	M	23	1.20	3.40	0.47	0.41	0.28	1.76	0.104	1.11
LAB22	F	27	-0.40	0.40	0.47	0.41	0.27	1.49	0.116	0.67
LAB23	F	26	0.90	4.80	0.49	0.36	0.30	1.99	0.086	1.21
LAB24	M	21	-0.20	0.00	0.52	0.47	0.38	1.59	0.106	0.64
LAB25	M	26	0.50	2.20	0.38	0.26	0.25	1.67	0.108	0.91
LAB26	M	23	2.00	3.00	0.38	0.38	0.30	1.76	0.095	2.59
LAB27	M	28	-0.50	1.20	0.40	0.38	0.28	1.62	0.091	0.95
LAB28	F	26	-0.40	3.10	0.51	0.45	0.35	1.91	0.101	0.97
LAB29	F	22	0.00	3.50	0.43	0.47	0.27	1.79	0.098	0.90
LAB30	F	28	1.20	2.70	0.27	0.36	0.34	1.85	0.093	0.82
Mean		24.97	0.26	2.66	0.43	0.42	0.29	1.84	0.096	1.07
STD		2.76	0.82	1.23	0.07	0.08	0.04	0.18	0.011	
CIEPO06 standard			0.00	0.00	0.38	0.38	0.30	1.76	0.095	

Optics EXPRESS

Table 11. The 2° parameters for the 4 young observers using two methods.

Gender	Method	Age	L_{shift}	M_{shift}	l_{OD}	m_{OD}	s_{OD}	k_{lens}	k_{mac}
F	RGB	21	-0.40	3.80	0.36	0.41	0.40	1.46	0.353
	Lab	21	0.30	3.60	0.49	0.45	0.37	1.84	0.423
F	RGB	29	-0.10	4.00	0.49	0.42	0.35	2.05	0.414
	Lab	29	0.40	3.80	0.59	0.59	0.36	1.83	0.389
M	RGB	28	0.20	3.50	0.49	0.44	0.35	2.03	0.451
	Lab	28	-0.10	3.00	0.38	0.67	0.38	1.77	0.437
M	RGB	30	0.40	2.80	0.40	0.50	0.37	1.66	0.269
	Lab	30	-0.50	1.60	0.40	0.41	0.32	1.97	0.428
CIE	PO06	.	.00	0.00	0.50	0.50	0.40	1.76	0.350

Table 12. The 10° parameters for the 4 young observers using two methods.

Gender	Method	Age	L_{shift}	M_{shift}	l_{OD}	m_{OD}	s_{OD}	k_{lens}	k_{mac}
F	RGB	21	-0.40	3.80	0.32	0.40	0.38	1.46	0.097
	Lab	21	0.30	3.60	0.35	0.33	0.29	1.84	0.107
F	RGB	29	-0.10	4.00	0.51	0.45	0.37	2.05	0.112
	Lab	29	0.40	3.80	0.49	0.42	0.37	1.83	0.098
M	RGB	28	0.20	3.50	0.49	0.56	0.33	2.03	0.089
	Lab	28	-0.10	3.00	0.41	0.25	0.32	1.77	0.110
M	RGB	30	0.40	2.80	0.36	0.29	0.25	1.66	0.109
	Lab	30	-0.50	1.60	0.43	0.52	0.21	1.97	0.090
CIE	PO06		0.00	0.00	0.38	0.38	0.30	1.76	0.095

Funding. National Natural Science Foundation of the Chinese government (61775190); Biotechnology and Biological Sciences Research Council.

Disclosures. The authors declare no conflicts of interest.

Data availability. Data underlying the results presented in this paper are not publicly available at this time but may be obtained from the authors upon reasonable request.

References

1. CIE, "Fundamental chromaticity diagram with physiological axes – part 1," (2006).
2. CIE, "Fundamental chromaticity diagram with physiological axes – part 2: spectral luminous efficiency functions and chromaticity diagrams," (2015).
3. A. Stockman and L. T. Sharpe, "Cone spectral sensitivities and color matching," in K. Gegenfurtner and L. T. Sharpe eds., *Color Vision: From Genes to Perception (Pp. 53-87)* (Cambridge University Press, Cambridge 1999), pp. 53–87.
4. A. Stockman, L. T. Sharpe, C. Fach, *et al.*, "The spectral sensitivity of the human short-wavelength sensitive cones derived from thresholds and color matches," Vision Res. **39**(17), 2901–2927 (1999).
5. W. S. Stiles and J. M. Burch, "NPL colour-matching investigation: final report," Opt. Acta **6**(1), 1–26 (1959).
6. N. I. Speranskaya, "Determination of spectral colour co-ordinates for twenty-seven normal observers," Opt. Spectrosc **7**, 424–428 (1959).
7. K. Shi, M. R. Luo, A. Rider, *et al.*, "The age effect on observer colour matching and individual colour matching functions," *Color and Imaging Conference* (2023).
8. P. L. Webster and R. D. MacLeod, "Characteristics of root apical meristem cell population kinetics: a review of analyses and concepts," Environ. Exp. Bot. **20**(4), 335–358 (1980).
9. B. Oicherman, "Effects of colorimetric additivity failure and of observer metamerism on cross-media colour matching," Department of Colour Science University of Leeds, (2007).
10. P. Morvan, A. Sarkar, J. Stauder, *et al.*, "A handy calibrator for color vision of a human observer," in *2011 IEEE International Conference on Multimedia and Expo* (2011), pp. 1–4.
11. A. Sarkar, "Identification and assignment of colorimetric observer categories and their applications in color and vision sciences," Signal and Image processing (2011).
12. Y. Asano, "Individual colorimetric observers for personalized color imaging," (n.d.).

Optics EXPRESS

13. Y. Asano, "Multiple color matches to estimate human color vision sensitivities," *International Conference on Image and Signal Processing* (2014).
14. J. Wu, M. Wei, Y. Fu, *et al.*, "Color mismatch and observer metamerism between conventional liquid crystal displays and organic light emitting diode displays," Opt. Express **29**(8), 12292 (2021).
15. K. Shi and M. R. Luo, "Factors affecting colour matching between displays," Opt. Express **30**(15), 26841–26855 (2022).
16. M. Ko, Y. Kwak, G. Seo, *et al.*, "Reducing the CIE colorimetric matching failure on wide color gamut displays," Opt. Express **31**(4), 5670 (2023).
17. K. Shi, M. R. Luo, A. Rider, *et al.*, "A multi-primary trichromator to derive individual color matching functions and cone spectral sensitivities," Color Res. Appl. (2023).
18. J. Guild, "The colorimetric properties of the spectrum," Philosophical Transactions of the Royal Society of London. Series A, Containing Papers of a Mathematical or Physical Character Series A **230**, 149–187 (1931).
19. W. D. Wright, "A re-determination of the mixture curves of the spectrum," Trans. Opt. Soc. **31**(4), 201–218 (1930).
20. J. C. Maxwell, "On the theory of compound colours and the relations of the colours of the spectrum," Philos. Trans. R. Soc. London **150**, 57–84 (1860).
21. H. Grassman, "On the theory of compound colours," The London, Edinburgh, and Dublin Philosophical Magazine and Journal of Science **7**(45), 254–264 (1854).
22. B. H. Crawford, "Color matching and adaptation," Vision Res. **5**(1-3), 71–78 (1965).
23. G. Wyszecki and W. S. Stiles, *Color Science: concepts and methods, quantitative data and formulae (2nd ed.)*, John wiley & sons (2000).
24. Q. Zaidi, "Adaptation and color matching," Vision Res. **26**(12), 1925–1938 (1986).
25. Y. Asano, M. D. Fairchild, L. Blondé, *et al.*, "Color matching experiment for highlighting interobserver variability," Color Res. Appl. **41**(5), 530–539 (2016).
26. R. S. Berns, R. J. Motta, M. E. Gorzynski, *et al.*, "CRT colorimetry. part I: Theory and practice," Color Res. Appl. **18**(5), 299–314 (1993).
27. L. M. Hurvich, "Color Vision," MA: Sinauer Associates Sunderland, 222–229 (n.d.).
28. A. Stockman and A. Rider, "Formulae for generating standard and individual human cone spectral sensitivities," Color Res. Appl. (2023).
29. M. R. Luo, G. Cui, B. Rigg, *et al.*, "The development of the CIE 2000 colour-difference formula: CIEDE2000," Color Res. Appl. **26**(5), 340–350 (2001).
30. J. Neitz and M. Neitz, "The genetics of normal and defective color vision," Vision Res. **51**(7), 633–651 (2011).
31. J. Winderickx, L. Battlsti, Y. Hlbiya, *et al.*, "Haplotype diversity in the human red and green opsin genes: evidence for frequent sequence exchange in exon 3," Hum Mol Genet **2**(9), 1413–1421 (1993).
32. A. Stockman and L. T. Sharpe, "The spectral sensitivities of the middle- and long-wavelength-sensitive cones derived from measurements in observers of known genotype," Vision research (Oxford) **40**(13), 1711–1737 (2000).
33. L. T. Sharpe, A. Stockman, H. Jägle, *et al.*, "Red, Green, and Red-Green Hybrid Pigments in the Human Retina: Correlations between Deduced Protein Sequences and Psychophysically Measured Spectral Sensitivities," J. Neurosci. **18**(23), 10053–10069 (1998).
34. G. Jordan, S. S. Deeb, J. M. Bosten, *et al.*, "The dimensionality of color vision in carriers of anomalous trichromacy," Journal of Vision **10**(8), 12 (2010). doi:10.1167/10.8.12
35. G. Jordan and J. Mollon, "Tetrachromacy: the mysterious case of extra-ordinary color vision," Current Opinion in Behavioral Sciences **30**, 130–134 (2019).